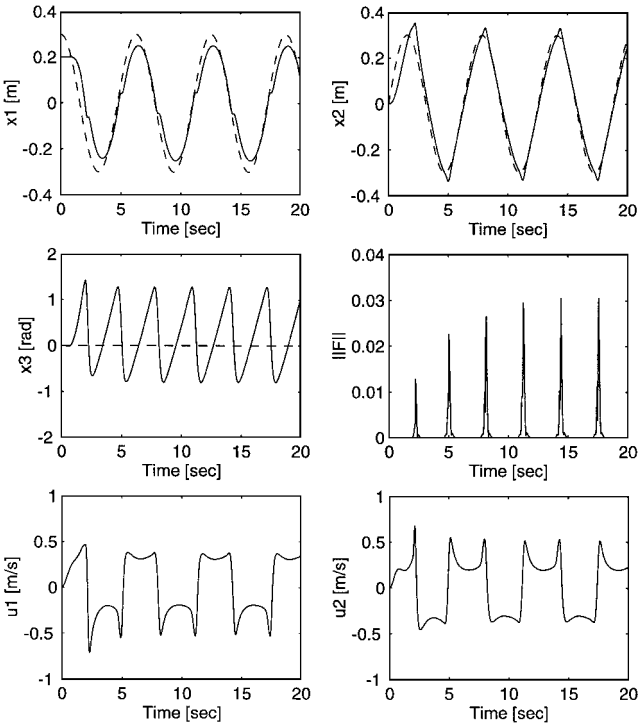

Fig. 1 Time histories of a simulation result with T_f = 1 s and Q = diag(10, 10, 0.1): – – –, reference state and ——, actual state.

has bounded magnitude. The system is controlled by the bounded control input so as to minimize the deviation from the desired reference trajectory on average over $[t, t + T]$. Because the system is nonholonomic and cannot track the reference trajectory given by Eq. (26) perfectly with any control input, the performance index is not bounded with respect to the time interval T and an infinite horizon regulator cannot be designed for the present tracking control problem. However, the receding-horizon tracking control can be designed because of the finite T.

The initial state is given in the simulation as $x_1 = 0.2$ m, $x_2 = 0$ m, and $x_3 = 0$ rad. The parameters are chosen as $L = 0.0605$ m, $R_0 = 0.3$ m, $\omega_0 = 1.0$ rad/s, and $\alpha = 0.5$. The matrix to stabilize the solution is chosen as $A_s = -50I$. The Adams method starting with the Runge–Kutta–Gill method is used for numerical integration of the differential equations on both the t axis and the τ axis. The time step on the t axis is 0.01 s, and the time step on the τ axis is 0.05 s. The simulation program is coded in C language on an Apple Power Macintosh 7100/80AV (CPU: PowerPC 601, 80 MHz; RAM: 32 MB), and the size of the binary file of the program is 66 KB. The whole computational time is about 15 s for simulating the control process of 20 s. Therefore, it can be concluded that the proposed control algorithm is implemented with a sufficiently short computational time and a moderate amount of data storage. The computational time can be reduced further by changing the integration method and/or the time steps at the expense of accuracy.

The simulation result in Fig. 1 is a case with $T_f = 1$ s and Q = diag(10, 10, 0.1). Time histories of state variables; the norm of the error in the optimality condition, $\|\boldsymbol{F}\|$; and control inputs are shown in Fig. 1. The error $\|\boldsymbol{F}\|$ is less than 0.04 throughout the simulation, which validates the accuracy of the optimal solution. The peaks of $\|\boldsymbol{F}\|$ appear when the attitude angle x_3 changes rapidly. The attitude angle x_3 vibrates around the constant reference state of zero because the model cannot move in the x_1 direction with zero attitude angle. Optimization results in satisfactory tradeoff between tracking performance of x_1, x_2, and x_3. The closed-loop performance depends on free parameters of the performance index in the present optimization-based control.

Conclusions

An algorithm is proposed for the time-variant receding-horizon control of general nonlinear systems. The algorithm is derived in a manner that is different from the conventional one, and it is shown that the unknown costate is governed by a differential equation that is a natural extension of the Euler–Lagrange equations for a usual finite horizon optimal control problem with a fixed terminal time. A tracking control problem of a two-wheeled car is employed as a numerical example. It is shown that the proposed algorithm requires a realistic amount of computational time and data storage in the simulation. As the result of the numerical simulation, it is concluded that the receding-horizon tracking control achieves the best possible performance even if the reference trajectory cannot be tracked perfectly with any control input. The present approach can generate a highly nonlinear control law through optimization requiring trial and error only in selection of a few free parameters. It may be concluded that the present approach provides an efficient design technique for a wide class of nonlinear feedback control problems.

Acknowledgments

This work was partially supported by the Research Fund of the CASIO Science Promotion Foundation. The author thanks the anonymous reviewers for valuable comments.

References

[1] Ohtsuka, T., and Fujii, H. A., "Real-Time Optimization Algorithm for Nonlinear Receding-Horizon Control," *Automatica*, Vol. 33, No. 6, 1997, pp. 1147–1154.

[2] Michalska, H., "Trajectory Tracking Control Using the Receding Horizon Strategy," *Proceedings of International Workshop on Predictive and Receding Horizon Control*, Engineering Research Center for Advanced Control and Instrumentation, Seoul National Univ., Seoul, Republic of Korea, 1995, pp. 1–12.

[3] Bryson, A. E., Jr., and Ho, Y.-C., *Applied Optimal Control*, Hemisphere, New York, 1975, Secs. 2.3 and 6.3.

[4] Ohtsuka, T., "Time-Variant Receding-Horizon Control of Nonlinear Systems," AIAA Paper 96-3694, July 1996.

Intercept of Nonmoving Targets at Arbitrary Time-Varying Velocity

Ping Lu*
Iowa State University, Ames, Iowa 50011-3231

I. Introduction

PROPORTIONAL navigation (PN) guidance has been probably the most popular and extensively studied guidance method for short-range intercept. Pastrick et al.[1] provide a historical background of the PN guidance concept and a comprehensive list of the literature on PN guidance laws up to 1979. Many additional publications have since appeared on PN guidance and its variations.[2–5] In almost all of the existing studies where the capture of the target with PN guidance is analytically investigated, a key assumption is that the interceptor and the target have constant velocities. The PN guidance law in principle has no difficulty being applied to long-range intercept. For instance, in the entry flight of a lifting space vehicle, the vehicle needs to be guided from the penetration of the atmosphere to a target point near the landing site where final approach and landing maneuvers are initiated.[6] However, when the PN guidance law is applied to such a long-range intercept, the constant-velocity assumption is no longer a valid approximation because the velocity variation in this case can be as large as one order of magnitude. In this Note, we examine the PN guidance law applied to the intercept of a nonmoving target when the interceptor has arbitrary time-varying velocity. We shall show that the PN guidance law will

Received June 4, 1997; revision received July 31, 1997; accepted for publication Sept. 19, 1997.

*Associate Professor, Department of Aerospace Engineering and Engineering Mechanics. E-mail: plu@iastate.edu. Associate Fellow AIAA.

lead to intercept of the target for any initial conditions, except for the case when the interceptor is moving away from the target along the negative direction of the line of sight.

II. Guidance Law and Analysis of Intercept

We shall consider intercept in the horizontal plane while the interceptor can be in three-dimensional motion over a flat Earth. This would be the case for entry vehicle guidance where the longitudinal (vertical) flight is guided by a different scheme,[6] and the lateral guidance logic is responsible for guiding the vehicle to the target point location. Let the coordinate system oxy in the horizontal plane, shown in Fig. 1, be centered at the nonmoving target with the x axis pointing toward the east and the y axis north. The kinematics of the interceptor in the horizontal plane are then given by

$$\dot{x} = V_T(t)\cos\gamma(t)\sin\psi(t) \tag{1}$$

$$\dot{y} = V_T(t)\cos\gamma(t)\cos\psi(t) \tag{2}$$

where V_T is the total velocity of the interceptor, γ is the flight-path angle of the interceptor, and ψ is the velocity azimuth angle of the interceptor, measured in the horizontal plane from the north in a clockwise direction. Note that $V_T(t)$, as well as $\gamma(t)$, is generally time varying and affected by gravity, propulsion, if any, and aerodynamic forces. We will allow arbitrary variations of $V_T(t) > 0$ and $\gamma(t) \in (-\pi/2, \pi/2)$ and simply denote $V(t) = V_T(t)\cos\gamma(t)$. The azimuth angle of the line of sight from the interceptor to the target is ψ^*, and

$$\psi^* = \tan^{-1}(-x/-y) \tag{3}$$

The negative signs are added for determination of the appropriate quadrant of ψ^*. The time derivative of ψ^* is obtained with the aid of Eqs. (1–3):

$$\dot{\psi}^* = V(t)\left(\frac{y\sin\psi - x\cos\psi}{x^2 + y^2}\right) \tag{4}$$

The guidance law is a PN law in which ψ is commanded by

$$\dot{\psi} = \lambda\dot{\psi}^* \tag{5}$$

for some constant λ, the range of which is to be determined. Suppose that the initial conditions θ_0 and ψ_0 are restricted in the range of $[0, 2\pi]$. Then for any $r_0 > 0$, θ_0 and ψ_0 such that $\psi_0 + \theta_0 \neq \pi/2$ or $5\pi/2$, we have the following results.

1) For any $\lambda > 1$ and $\neq 2$ in Eq. (5), the separation r between the interceptor and the target point will asymptotically approach zero.

2) When $\lambda = 2$, $r = 0$ will occur in a finite time.

3) For any $\lambda > 2$ the intercept trajectory will end in a direct collision course with $\dot{\theta} \to 0$ and $\dot{\psi}^* \to 0$.

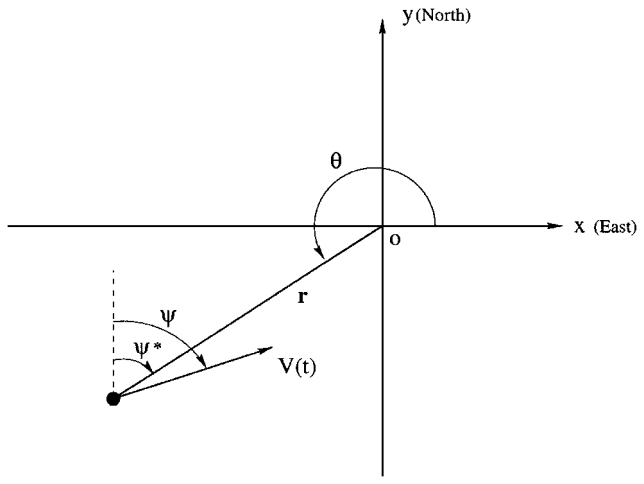

Fig. 1 Intercept geometry in horizontal plane.

Let us show how these results are obtained. We first eliminate the explicit dependence on the arbitrary (positive) time function $V(t)$ by introducing a new independent variable:

$$\tau = \int_0^t V(\sigma)\,\mathrm{d}\sigma \tag{6}$$

or

$$\mathrm{d}\tau = V(t)\,\mathrm{d}t \tag{7}$$

Then, Eqs. (1), (2), and (5) become

$$\frac{\mathrm{d}x}{\mathrm{d}\tau} = x' = \sin\psi \tag{8}$$

$$\frac{\mathrm{d}y}{\mathrm{d}\tau} = y' = \cos\psi \tag{9}$$

$$\frac{\mathrm{d}\psi}{\mathrm{d}\tau} = \psi' = \frac{\lambda(y\sin\psi - x\cos\psi)}{x^2 + y^2} \tag{10}$$

It is more convenient to use polar coordinates $r = \sqrt{(x^2 + y^2)}$ and θ, as shown in Fig. 1. In terms of r and θ, the preceding equations are equivalent to

$$r' = \sin(\psi + \theta) \tag{11}$$

$$\theta' = \frac{\cos(\psi + \theta)}{r} \tag{12}$$

$$\psi' = -\lambda\frac{\cos(\psi + \theta)}{r} \tag{13}$$

Define

$$\phi = \psi + \theta \tag{14}$$

The system (11–13) reduces to

$$r' = \sin\phi \tag{15}$$

$$\phi' = (1 - \lambda)(\cos\phi/r) \tag{16}$$

Eliminating the dependence on τ between Eqs. (15) and (16) gives

$$\frac{\mathrm{d}r}{\mathrm{d}\phi} = \frac{r\tan\phi}{1 - \lambda} \tag{17}$$

Integrating this equation yields

$$r = C|\cos\phi|^{1/(\lambda - 1)} \tag{18}$$

where $C > 0$ is an integration constant. Consider for the moment the case where $\cos\phi > 0$. Substitute Eq. (18) into Eq. (16) to have

$$\phi' = [(1 - \lambda)/C](\cos\phi)^{(\lambda - 2)/(\lambda - 1)} \tag{19}$$

For any $\lambda > 1$, Eq. (19) indicates that $\phi' < 0$. Thus, ϕ will monotonically decrease, approaching $\phi = -\pi/2$ if $-\pi/2 < \phi_0 < \pi/2$ or $\phi \to 3\pi/2$ if $3\pi/2 < \phi_0 < 5\pi/2$. In particular, when $\lambda = 2$, ϕ will decrease linearly to $-\pi/2$ or $3\pi/2$, depending on ϕ_0, in a final time $\tau_f = C(\pi/2 + \phi_0)/(\lambda - 1)$ or $C(\phi_0 - 3\pi/2)/(\lambda - 1)$. When $\lambda > 2$, $\phi' \to 0$ as $\phi \to -\pi/2$ (or $3\pi/2$). Therefore $\psi^{*\prime} = -\phi'/(1 - \lambda) \to 0$ and $\theta' = \phi'/(1 - \lambda) \to 0$, which suggests that $\dot{\psi}^*$ and $\dot{\theta} \to 0$. In all cases, $r \to 0$ by Eq. (18), or $r = 0$ at τ_f when $\lambda = 2$.

For the case where $\cos\phi < 0$, a negative sign is added to the right-hand side of Eq. (19) and $\cos\phi$ is replaced by $-\cos\phi$. Similar arguments will show that ϕ will monotonically increase to $3\pi/2$ or $5\pi/2$. The proof of the rest of the stated results then follows. The only case where interception will not occur is when $\phi_0 = \psi_0 + \theta_0 = \pi/2$ or $5\pi/2$. This is the case when the interceptor is moving away from the target along the negative direction of the line of sight.

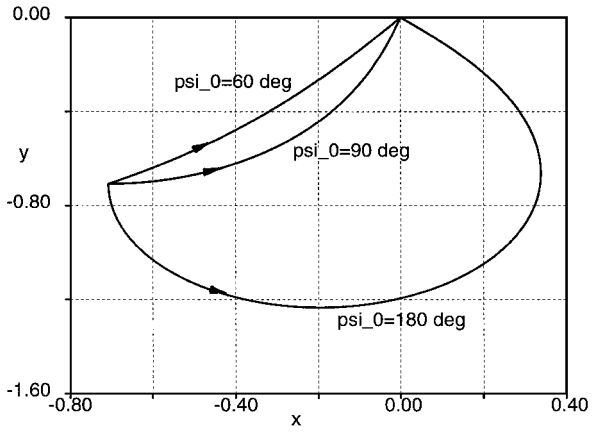

Fig. 2 Trajectories with different initial $\psi(0)$.

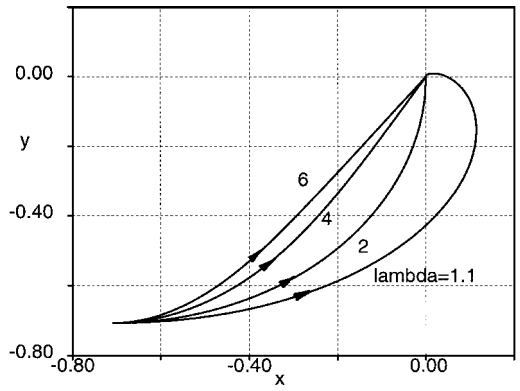

Fig. 3 Trajectories with different λ values.

Remarks:

1) Although theoretically r will not reach zero in finite time (except for $\lambda = 2$), simulations reveal that r always reaches a very small value (practically zero) in finite times.

2) The property that $\dot{\psi} = \lambda\dot{\psi}^* \to 0$ for $\lambda > 2$ is desirable. This means that the required turning acceleration of the interceptor in the horizontal plane, $V_T\dot{\psi}$, is approaching zero near the end.

3) Similar results are obtained in Ref. 7 for constant-velocity interceptor and target. Specifically, it can be deduced from Ref. 7 that $\lambda > 1$ is required for a constant-velocity interceptor to capture a target if the target is stationary. Also, applying the discussion in Ref. 7 to a nonmoving target yields that for $\lambda > 2$ the line-of-sight (LOS) rotation rate is decreasing near the end, although the conclusion of the vanishing LOS rotation rate is not readily available from Ref. 7.

4) The conclusions obtained in this Note are independent of the actual variations of the interceptor velocity $V_T(t)$ and flight-path angle $\gamma(t)$. This enables the guidance algorithm in the vertical direction, which will result in changes in γ, to function independently.

Figure 2 shows the intercept trajectories based on Eqs. (8–10) for $\lambda = 2.5$ with different $\psi(0)$ values and fixed dimensionless $r(0) = 1$ and $\theta(0) = 225$ deg, where x and y are normalized by $r_0 = \sqrt{[x^2(0) + y^2(0)]}$. Figure 3 contains the comparison of intercept trajectories for the fixed initial conditions $r(0) = 1$, $\theta(0) = 225$ deg, and $\psi(0) = 90$ deg as λ varies. It is seen that, the larger λ is, the more rapidly the trajectory will approach a direct collision course.

III. Conclusions

A PN guidance law is applied to an interceptor that has arbitrary time-varying velocity and is to reach a nonmoving target point. When the proportional constant is greater than unity, intercept will occur for all initial conditions, except for the case when the interceptor is moving away from the target initially along the LOS. When the proportional constant is greater than 2, the intercept will end in a direct collision course, with the required normal acceleration being zero for the interceptor.

Acknowledgments

This research has been supported by the NASA Marshall Space Flight Center under Grant NAG8-1289. The Technical Monitor is John M. Hanson.

References

[1]Pastrick, H. L., Seltzer, S. M., and Warren, M. E., "Guidance Laws for Short-Range Tactical Missiles," *Journal of Guidance and Control*, Vol. 7, No. 2, 1979, pp. 98–108.

[2]Rao, M. N., "New Analytical Solutions for Proportional Navigation," *Journal of Guidance, Control, and Dynamics*, Vol. 16, No. 3, 1993, pp. 591–594.

[3]Ghose, D., "On the Generalization of True Proportional Navigation," *IEEE Transactions on Aerospace Electronic Systems*, Vol. AES-30, No. 4, 1994, pp. 545–555.

[4]Zarchan, P., "Proportional Navigation and Weaving Targets," *Journal of Guidance, Control, and Dynamics*, Vol. 18, No. 5, 1995, pp. 969–974.

[5]Yang, C. D., and Yang, C. C., "Analytical Solution of Three-Dimensional Realistic True Proportional Navigation," *Journal of Guidance, Control, and Dynamics*, Vol. 19, No. 3, 1996, pp. 569–577.

[6]Harpold, J. C., and Graves, C. A., "Shuttle Entry Guidance," *Journal of the Astronautical Sciences*, Vol. 37, No. 3, 1979, pp. 239–268.

[7]Guelman, M., "A Qualitative Study of Proportional Navigation," *IEEE Transactions on Aerospace Electronic Systems*, Vol. AES-7, No. 4, 1971, pp. 637–643.

Matrix Symmetrization

I. Y. Bar-Itzhack*
Technion—Israel Institute of Technology, Haifa 32000, Israel

Introduction

THE role of Riccati and Lyapunov equations and their solutions in optimal control and Kalman filtering is well known.[1–3] It is also well known that the solution of these equations, which is a real symmetric matrix, loses its symmetry because of numerical errors. The simplest and most straightforward way to restore this property is symmetrization, which is performed at each instant in which the matrix is computed[4–6]; that is, if we denote by P the raw solution at a certain stage, then P is replaced by the matrix P_s, where

$$P_s = (P + P^T)/2 \tag{1}$$

In the ensuing we will refer to P_s as the symmetrized P.

Whereas the replacement of P by P_s is the obvious way to solve the problem, there may seemingly be better ways to restore symmetry. In particular, one may wish to replace P by the symmetric matrix that is the closest to it. This raises the question, what is the symmetric matrix that is the closest, in the Frobenius norm, to P? It turns out that the real symmetric matrix closest to P is the symmetrized P. Although proven in 1955 (Ref. 7), this fact is not widely known. The purposes of this Note are, first, to bring this fact to the attention of the readers; second, to present a new proof that is different from that presented in Ref. 7; and finally, to show that this result can be explained in a rather simple manner.

Closest Symmetric Matrix

Next we prove the fact that P_s is P_c, where P_c denotes the $n \times n$ symmetric matrix closest to the $n \times n$ P matrix. The following theorem and proof are according to Ref. 7.

Theorem: The closest symmetric matrix to a real matrix, in Frobenius (Euclidean) norm, is its symmetrized matrix.

Received April 7, 1997; revision received July 2, 1997; accepted for publication Sept. 13, 1997.

*Sophie and William Shamban Professor of Aerospace Engineering, Faculty of Aerospace Engineering, and Member, Technion Space Research Institute. E-mail: ibaritz@tx.technion.ac.il. Associate Fellow AIAA.